Ecotoxicology and Environmental Safety 162 (2018) 245–252

Contents lists available at ScienceDirect

Ecotoxicology and Environmental Safety

journal homepage: www.elsevier.com/locate/ecoenv

Synthesis of novel magnetic nano-sorbent functionalized with N-methyl-D-glucamine by click chemistry and removal of boron with magnetic separation method

Servet Tural[a,*], Mehmet Şakir Ece[a,b], Bilsen Tural[a]

[a] Department of Chemistry, Faculty of Education, Dicle University, 21280 Diyarbakir, Turkey
[b] Vocational High School of Health Services, Mardin Artuklu University, 47100 Mardin, Turkey

ARTICLE INFO

Keywords:
Boron
Click chemistry
Magnetic separation method
Nano-sorbent
Sorption

ABSTRACT

Click chemistry refers to a group of reactions that are fast, simple to use, easy to purify, versatile, regiospecific, and give high product yields. Therefore, a novel, efficient magnetic nano-sorbent based on N-methyl-D-glucamine attached to magnetic nanoparticles was prepared using click coupling method. Its boron sorption capacity was compared with N-methyl-D-glucamine direct attached nano-sorbent. The characterization of the magnetic sorbents was investigated by several techniques such as X-ray diffraction, scanning electron microscope, transmission electron microscope, dynamic light scattering, thermogravimetric analysis, Fourier transform infrared spectrophotometer, and vibrating sample magnetometer. The boron sorption capacity of sorbents was compared by studying various essential factors influencing the sorption, like sorbate concentration, sorbents dosage, pH of the solution, and contact time. Langmuir and Freundlich and Dubinin-Radushkevich adsorption isotherms models were applied. Percent removal and sorption capacities efficiencies of sorbents obtained with direct and click coupling are found to be 49.5%, 98.7% and 6.68 mg/g, 13.44 mg/g respectively. Both sorbents have been found to be compatible with Langmuir isotherm, and the boron sorption kinetics conforms to the pseudo second order kinetics. The reusability study of sorbents was carried out five times for boron sorption and desorption.

1. Introduction

Boron pollution in the water is a common problem for the environment. Depending on the pH of the solution, boron is present in two forms (Boric acid ($B(OH)_3$) and borate anions ($B(OH)_4^-$)) (Sabarudin et al., 2005) . Since no specific biochemical function was defined in human nutrition, boron was not found to be an important element in the human diet. However, boron is important in human physiology in responding to vitamin D and calcium-magnesium metabolism and use, improving brain function, psychomotor response, and estrogen response in postmenopausal women. Boron has a role in healthy bones (Devirian and Volpe, 2003).

There was no maximum limit of boron for drinking water in the US; however, in the US, EPA (Environmental Protection Agency) has established the standard for boron drinking waters as 0.6 mg BL^{-1}. Although there is no general subsumption and there are different values that vary from country to country, a limit of 0.3 mg/L (after that revised to 0.5 mg/L) was determined by the World Health Organization (WHO) for boron in drinking water (Liu et al., 2009c). Then, this limit value was revised by the same organization to 2.4 mg/L in 2009 (Kluczka et al., 2015) Probably, 2.4 mg/L is an accepted value for humans. Since boron shows herbicidal activity, it still maintains 0.5 mg/L for irrigation water (Shah et al., 2017) otherwise, various plant species are highly susceptible to boron (Eg 1 mg/L, absolutely toxic dose for sunflower) (Kluczka et al., 2015). In spite of this value of the world health organization, many countries (Eg European Union, UK, Poland, South Korea, Singapore, and Japan) apply their own much lower limits (Wang et al., 2014).

Boron on useful plants and irrigation water sources is a particular concern because of its toxic effects. Its unique qualities are the extremely limited concentration band in suitable irrigation water at the growth of the plant. For activities related to metabolism in plants, there is a need for even a small concentration of boron in the irrigation water; however, a little higher desired concentration of the plant growth boron shows toxic effect. A yellowish stain on the leaves and in the foliage and acceleration of the decay process, and eventually the filling of the plant period is observed (Samatya et al., 2010).

Removing boron from water is difficult and not very practical and

* Corresponding author.
E-mail address: stural@dicle.edu.tr (S. Tural).

https://doi.org/10.1016/j.ecoenv.2018.06.066
Received 18 March 2018; Received in revised form 29 May 2018; Accepted 21 June 2018
Available online 11 July 2018

extremely expensive. There are many methods used to remove boron from aqueous solutions and sea water e.g. ion exchange, adsorption processes, precipitation and membrane processes (electrodialysis reversal and reverse osmosis) electrocoagulation. Among the methods used for boron removal, the methods in which boron selective resins are used are the most effective ones (Guan et al., 2016; Samatya et al., 2015).

In the recent years, there is a growing interest in the use of magnetic nanoparticles (MNPs) based on magnetic assisted separation techniques (MAT) as an alternative to filtration or centrifugation separation methods (Anastopoulos et al., 2018; Kyzas and Matis, 2015). During the MAT process, functionalized MNPs are distributed as samples which contain target compounds, and thereafter the functionalized groups of surface's compounds perform the adsorption. After this process, the magnetic particles containing the adsorbed compounds are collected quickly by using an external magnet for separation. Using an external magnet is more efficient and selective than filtration processes or centrifugation (Anastopoulos et al., 2018; Kyzas and Matis, 2015; Tural, 2010).

Click chemistry is an approach that uses efficient, effective and reliable reactions to bind two molecular building blocks, such as Cu (I) catalyzed azide-alkyne cycloaddition (Mandoli, 2016; Singh et al., 2016). It expresses a group of reactions with these possibilities that are fast, simple to use, specific, easy to purify, high product yield, versatile regional (Mandoli, 2016; Singh et al., 2016). It has found applications in a wide variety of research areas, pharmaceutical sciences, materials science, polymer chemistry (Mandoli, 2016; Singh et al., 2016; Yang et al., 2017). Click chemistry is also being applied to functionalize inorganic moieties to develop hybrid nanocomposites such as metal oxide nanoparticles, carbon nanotubes, etc. for high performance materials (Kantheti et al., 2015). 1,2,3-Triazole compounds have high solubility in aqueous solutions and do not react with functional groups at all. For this reason, the Huisgen 1,3-dipolar cycloaddition reaction are used in the synthesis of various polymeric carrier systems and dendrimers, in cross-linking of the grains, and in synthesis to modify the surfaces of various nanoparticle delivery systems (Hood et al., 2014). The click reactions are short-lived, highly efficient and highly selective reactions and the resulting triazole compounds are also stable compounds (Liebert et al., 2006; Link and Tirrell, 2003; Seo et al., 2003; Wang et al., 2003; Werz and Seeberger, 2005). These properties make ideal use of triazole compounds in the field of material science.

In this context, our aim is to develop a novel magnetic sorbent material for boron removal. To this end, magnetic silica was functionalized with N-methylglucamine via click-chemistry and direct coupling and the magnetic sorbents were tested for their efficiency the boron sorption in aqueous solutions. The equilibrium and kinetics of sorption of boron are investigated by two magnetic sorbents. To the best of our knowledge, there is no study relating N-methylglucamine functionalized onto magnetic silica nanoparticles via click-chemistry which is compared with direct coupling for removing boron from aqueous solutions.

2. Materials and methods

2.1. Chemicals and reagents

Boric acid (H_3BO_3), N-methyl-D-glucamine ($C_7H_{17}NO_5$), tetrahydrofuran (C_4H_8O) and dimethylformamide (C_3H_7NO) were purchased from Fluka Chemical Companies. Chloroform ($CHCl_3$) and iron (III) chloride hexahydrate ($FeCl_3{\cdot}6H_2O$) were supplied by MERCK Chemical Companies. Azomethine-H monosodium salt hydrate ($C_{17}H_{12}NNaO_8S_2{\cdot}aq$) provided from SIGMA Chemical Companies. Sodium azide (NaN_3), methylpropiolate ($HC{\equiv}CCO_2CH_3$), tetraethylorthosilicate ($C_8H_{20}O_4Si$), (3-bromopropyl) trimethoxysilane ($C_6H_{15}BrO_3Si$), N,N,N′,N″,N″-pentamethyldiethylenetriamine ($C_9H_{23}N_3$) were obtained from ALDRICH Chemical Companies. Citric acid monohydrate ($(HOC(COOH)(CH_2COOH)_2{\cdot}H_2O$), dichloromethane ($CH_2Cl_2$), diethyl ether $(C_2H_5)_2O$, ethanol (C_2H_5OH), acetic acid (CH_3COOH), copper (I) bromide (CuBr), L-(+)-ascorbic acid ($C_6H_8O_6$), iron (II) chloride tetrahydrate ($FeCl_2$), 2-propanol ($(CH_3)_2CHOH$) and sodium citrate tribasic dihydrate ($HOC(COONa)(CH_2COONa)_2{\cdot}2H_2O$) were supplied by SIGMA-ALDRICH Chemical Companies. The chemical substances and solvents used in the experiments are of analytical purity. As inert gas, 99.99% pure argon gas was used and obtained from Linde Companies.

2.2. Characterization

Morphology and particle size of silica coated magnetic nanoparticles (M-SiO_2) functionalized with N-methyl-D-glucamine (NMDG) using direct (M-NMDG) and clikc coupling (M-TACA) reaction were analyzed by a JEOL 2100 F transmission electron microscopy (TEM) (Japan). MNPs were dispersed at the required amount in water (distilled, deionized) by sonication for 10 s and these samples for TEM were placed on a Copper Grids (SPI Double-100/200). The morphology of the MNPs was investigated by a Field Emission Scanning Electron Microscopy (Quanta 400 F, FE-SEM (FEI)). Fourier Transform Infrared (FT-IR) spectra (sixteen scans (resolution = 4 cm^{-1})) were measured on a Nicolet FTIR (Thermoscientific, IS-10, USA) spectrophotometer. Agglomeration and the particle size distributions of the MNPs were determined using a Malvern Mastersizer 2000 (England). Magnetizations were measured using a cryogenic magneto-meter (Quantum Design PPMS-9T) at 25 °C. Thermogravimetric analysis (TGA) and differential thermal analysis (DTA) curves were obtained in N_2 atmosphere at a heating rate of 10 °C/min with a Shimadzu DTG-60 (Japan).

2.3. Synthesis of boron selective magnetic-sorbent via direct coupling

Details for synthesis and characterization of magnetic nanoparticles (MNPs) were described in our previous works (Tural et al., 2013). The functionalization of MNPs with NMDG via direct coupling was carried out in two stages. In the first stage, propyl bromide was linked to MNPs. In the next stage, NMDG was reacted with the resulting magnetic compound to obtain the tertiary amine functionalized particles. 1.0 g MNPs were diluted with acetic acid (0.01 M, 20 mL) and stirred (20 min). Immediately after this step, the particles were decanted by magnet; solution was evaluated as waste and the material left to dry at 120 °C for 24 h. The bromination of the MNPs was carried out overnight under an argon atmosphere and the reaction was carried out by refluxing with 1.0 g of MNPs in dry $CHCl_3$ (17 mL) solution with (3-bromopropyl) trimethoxysilane (0.75 mL). Brominated MNPs (M-SiO_2-Br) was obtained with a permanent magnet by magnetic separation and they were washed successively five times with a mixture of 10 mL of diethyl ether-dichloromethane (1:1), two times with 10 mL of chloroform and finally five times with 10 mL of deionized water. Then, the brominated MNPs were treated with 0.780 g of NMDG in reflux (10 mL water) for 24 h for binding of NMDG to the particles. In this last step, the final product was obtained by magnetic separation, the resulting particles were washed ten times with 15 mL deionized water and then the final product was dried on a lyophilizer. After all these steps NMDG functionalized MNPs (M-NMDG) was used as a magnetic sorbent for removal of boron from aqueous solutions. Each step in preparation of the magnetic nanoparticles is shown in Scheme 1.

2.4. Synthesis of boron selective magnetic-sorbent via click coupling

At this stage, synthesis of the resin was carried out based on the click chemistry. In the first step, the azide group was bound covalently to the M-SiO_2-Br particles (1.0 g) via a reaction between brominated MNPs and NaN_3 (0.75 g) in 15 mL of DMF at 50 °C for 24 h with continuous shaking. Then, 1.34 g of M-SiO_2-N_3 was added to a 100 mL two-necked balloon fitted with a reflux condenser. To this was added 15 mL

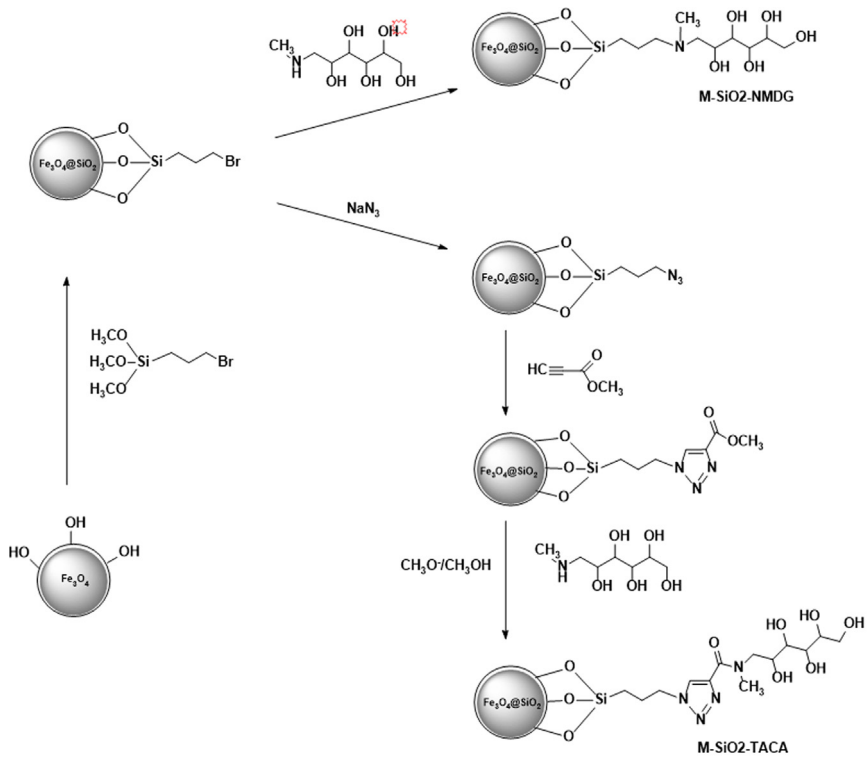

Scheme 1. Direct coupling and Click chemistry route for the covalent attachment of NMDG onto the magnetic silica nanoparticles.

of tetrahydrofuran (THF), 0.35 mL (4 mmol) of methyl propiolate, 460 mg (3.3 mmol) of CuBr and 0.66 mL (3.3 mmol) of pentamethyldiethylenetriamine (PMDTA). The reaction was maintained for 48 h at 40 °C inert gas atmosphere and 1.58 g of a product called M-TAC was obtained. The particles were washed 3 times with ethanol, 3 times with toluene and 3 times with ethanol (Wang et al., 2009). Then, 780 mg (4 mmol) NMDG and 20 mL of absolute methanol was added 100 mL three-necked flask. It was boiled under reflux for 20 min under argon atmosphere. 1.58 g of M-TAC was added. Immediately after, 0.1 mL of sodium methoxide (previously prepared in 25 mL absolute methanol solution which of containing 0.96 g (0.04 mol) of Na) solution was added. Under argon atmosphere, 40 mL of pure methanol was added in mixture. The mixture was boiled under reflux for 4 h. The resulting particles were washed 5 times with ethanol. Then, the particles were dried in a lyophilizer (Eggenhuisen et al., 2013). 2.12 g of sorbent called M-TACA was obtained. M-TACA synthesis reactions are shown in Scheme 1.

2.5. Boron removal with M-NMDG and M-TACA

Different sets of sorption experiments were carried out to investigate the effect of experimental conditions on the boron removal efficiency of the M-NMDG and M-TACA. To optimize the boron removal process, the effect of operating variables namely initial pH, initial boron concentration, sorbent dosage and time are studied. In the first set of experiments, the pH was varied in the range of 3.0–11.0 at a fixed boron concentration of 8.2 mg L^{-1}. The optimal pH identified from the first set of experiments was used for all the other studies. The influence of boron concentration on the removal efficiency was studied in the range of 2–128 mg L^{-1}. The effect of sorbent quantity was studied by mixing various amounts of M-NMDG and M-TACA sorbents (1.2–8.0 g L^{-1}) in conical flasks containing 2 mg L^{-1} boron solution at 30 °C for 30 min. Analysis of boron in sorption media was performed spectrophotometrically using the azomethine-H method (λ_{max}: 415 nm) (Tural, 2010).

The sorption capacity (Q) was calculated using Eq. (1):

$$Q = \frac{(C_i - C_f)V}{W} \tag{1}$$

where C_i is the initial concentration of boron (mg/mL); C_f is the final concentration of boron (mg/mL); V is the volume of boron solution (mL); and W is the weight of the used sorbents (g).

2.6. Batch kinetics and sorption isotherm models

A batch was used to describe the boron sorption kinetics on M-NMDG and M-TACA. Kinetic data showed that mass transfer and velocity control mechanism correlated with the linear form of the first-order Eq. (2) (Bhattacharya and Venkobachar, 1984):

$$\ln(Q_e - Q_t) = lnQ_e - k_1 t \tag{2}$$

and the second-order Eq. (3) (Ho, 2006):

$$\frac{t}{Q_t} = \frac{1}{(k_2 Q_e^2)} + \frac{t}{Q_e} \tag{3}$$

where Q_t and Q_e are the mass of boron (mg/g)N sorbed at time (t) and at equilibrium (e), respectively; k_2 (g/(mg min)) is the rate constant of the pseudo- second-order sorption and k_1 ($min-^1$) is the rate constant of the Pseudo-first-order sorption. With reference to Eq. (2), ln (Q_e-Q_t) gives a straight line giving a plot against t, a slope k_1 and a cut-off point lnQ_e. The plot of t/Q_t relative to t gives a straight line with $1/Q_e$ slope and $1/(k_2Q_e^2)$ section (Chen et al., 2011).

Three sorption isotherms models, namely Langmuir equation (Eq. (4)) (Langmuir, 1916), Freundlich equation (Eq. (5)) (Freundlich, 1906) and Dubinin–Radushkevich (D-R) equation (Eq. (6)) (Dubinin and Radushkevich, 1947) were used and these models are shown by the following equations:

$$\frac{1}{q_e} = \frac{1}{q_m b C_e} + \frac{1}{q_m} \tag{4}$$

$$log(q_t - q_e) = log(q_e) - \frac{k_1}{2.303} t \tag{5}$$

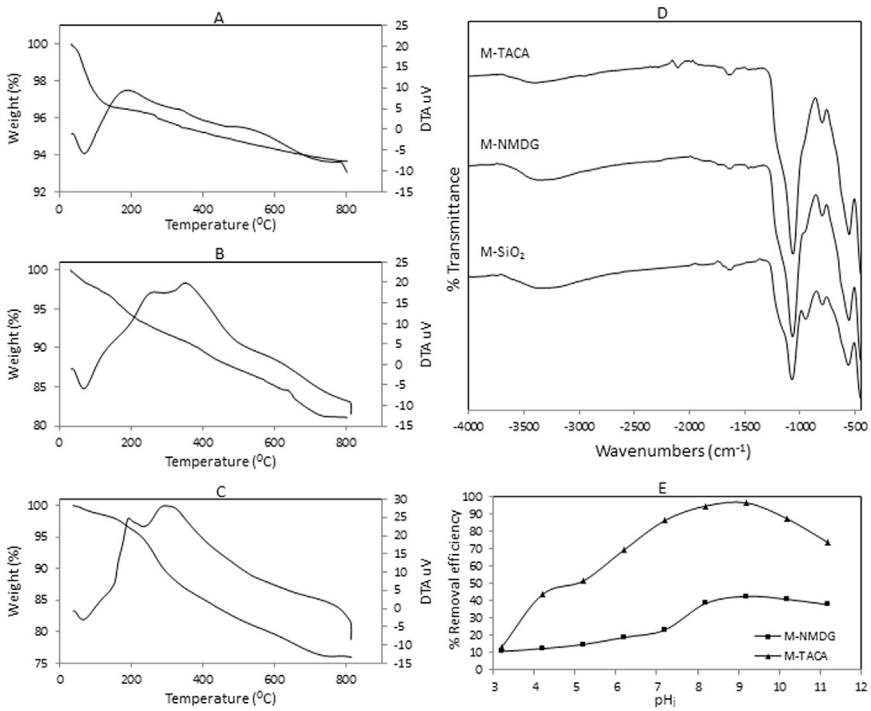

Fig. 1. A) TGA and DTA curves of M-SiO_2 **B)** TGA and DTA curves of M-NMDG **C)** TGA and DTA curves of M-TACA **D)** FT-IR spectrum of M-SiO_2, M-NMDG and M-TACA **E)** Effect of pH on sorption of boron onto M-NMDG and M-TACA (Sorbent dosage: 1.2 g/L, concentration of aqueous phase 8 mg/L boron, contact time: 30 min, stirring speed: 200 rpm, room temperature).

where q_e (mg/g) is the amount of boron sorption, qm (mg/g) is the maximum boron sorption capacity, C_e (mg/L) is the boron equilibrium concentration in solution, and b is Langmuir constant related to sorption capacity and energy of sorption.

The D-R equality definable with the undermentioned equation (Eq. (6)) (Dubinin, 1965; Dubinin and Radushkevich, 1947; Sing, 1982)

$$\ln q_e = \ln q_{max} - \beta\varepsilon^2 \tag{6}$$

where q_{max} is capacity of the theoretical saturation level, β is a constant related to energy of sorption, ε the Polanyi potential (mol^2/J^2), calculated from Eq. (7):

$$\varepsilon = RT\ln\left[1 + \frac{1}{C_e}\right] \tag{7}$$

wherein the solution temperature is T (K), R is the gas constant (8.314 J mol^{-1} K^{-1}) and Ce, sorbate (mg L^{-1}) is the equilibrium concentration, $\ln q_e$ by drawing by ε^2, the value of the β slope and the breakpoint q_{max} (mg g^{-1}) possible to determine the value, which is $\ln q_{max}$. The average value of E sorption free energy, E (kJ/mol), D-R parameter from B as expressed in the following equation B by using the values of the predictable (Eq. (8)) (Benhammou et al., 2005);

$$E = \frac{1}{\sqrt{2B}} \tag{8}$$

2.7. Desorption

In desorption experiments, constant (optimum) sorption conditions (pH = 8.2; C_0 = 8 mg/L; T = 30 °C; t = 30 min; Sorbent dosage = 1.2 g/L; Shaking speed = 200 rpm) were used in batch mode. The experiments were separated into two main categories: the first one was desorption pH-effect experiments, and the second one was reuse cycles with continuous sorption–desorption experiments. After the sorption stage, the sorbent materials were separated from supernatant by using an Nd–Fe–B permanent magnet. The separated sorbent particles were taken in flasks after being washed with deionized water as eluent with pH between 2.0 and 12.0. The desorption stage continued for 30 min. The best desorption results were obtained at pH 3.2 and desorption experiments were carried out at this pH. Desorption percentages were calculated by measuring the difference between the amount of boron removed in sorption stage and the amount of boron released in desorption stage. In order to find out the reusability of sorbents, the aforementioned process was repeated under the same conditions five more times.

3. Results and discussion

3.1. Characterization

The magnetic properties of the sorbents were investigated by VSM analysis at 25 °C. The saturation magnetization of M-NMDG and M-TACA (see Fig S1) was about 38.2 emug^{-1} and 37.0 emug^{-1}, respectively. As can be seen in Fig S1, there is a difference of 1.2 emug^{-1} between the magnetizations of the M-NMDG and M-TACA. Magnetization values of M-NMDG and M-TACA are suitable for magnetic separation (Frey et al., 2009; Hong et al., 2009; Lan et al., 2011; Xie et al., 2015).

Agglomerate sizes of the produced particles were analyzed by DLS by providing dispersions in water. For reliable results, each sample was distributed in the sonicator before analysis. Nano particles dimensional analysis results for M-SiO_2, M-NMDG and M-TACA with DLS are shown in Fig S2. As shown in the Fig S2, particles sizes of M-SiO_2, M-NMDG and M-TACA were approximately 479 nm, 724 nm and 832 nm, respectively. The most important factor that increases the agglomeration in aqueous solutions is the surface charge of the particles. Functional groups lead to changes in surface loads. Hence, 479 nm size of M-SiO_2 became 724 nm after being functionalized with NMDG. Due to the different surface charges, M-TACA has a grain size of 832 nm; thus, it is more agglomerated than M-NMDG (Cai et al., 2007; Gokce et al., 2014; Tural et al., 2016).

SEM images of M-NMDG and M-TACA are given in Fig S3-A and Fig S3-B, respectively. These images are similar spherical images, which confirm that sorbents surfaces morphologies are similar. As seen from the Fig S3-A and Fig S3-B, M-TACA has become more agglomerated than M-NMDG. This is consistent with DLS analysis results.

Thermal analysis results for M-SiO_2, M-NMDG and M-TACA are

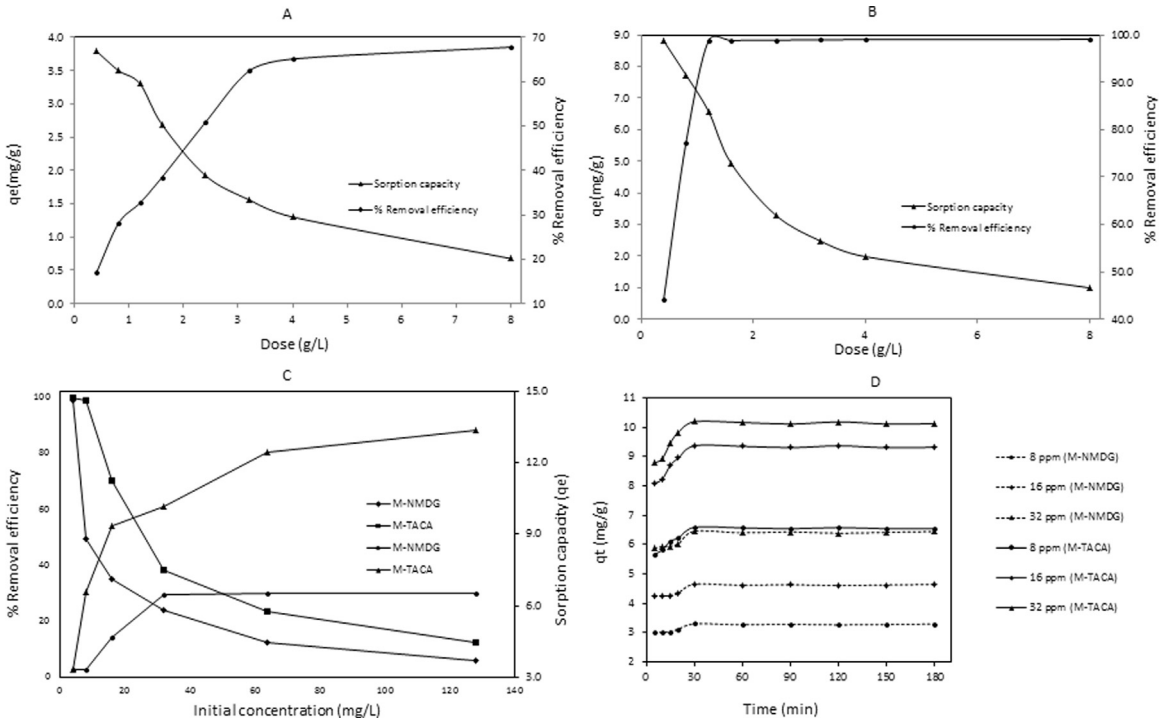

Fig. 2. A) The effect of M-NMDG dosage on the sorption capacity and boron removal percentages **B)** The effect of M-TACA dosage on the sorption capacity and boron removal (volume of the boron solution: 25 mL, pH: 8.2, contact time 30 min, stirring speed: 200 rpm, 30 °C) **C)** The effect of initial boron concentrations on the sorption capacity and boron removal percentages onto M-NMDG and M-TACA. **D)** The effect of time on sorption of boron at various concentrations onto M-NMDG and M-TACA (Sorbent dosage: 1.2 g/L, contact time: 30 min, stirring speed: 200 rpm, 30 °C).

given in Fig. 1-A, Fig. 1-B, Fig. 1-C, respectively. As seen in the Fig. 1(A, B, C), when the temperature is increased to 225 °C, a weight loss of about 4% is observed for all three samples (M-SiO_2, M-NMDG and M-TACA), which can be explained by the removal of water and organic volatiles. At elevated temperatures from 250 °C to 500 °C, two exothermic events are observed in the DTA curves of M-NMDG and M-TACA. These exothermic events come to fruition with a weight loss thought to be related to the burning of organic species. It is thought that the phase transition of the iron oxide particles occurs at the same temperature range (RĂILEANU et al., 2007; Ranjan and Brittain, 2007). The total weight losses of M-SiO_2, M-NMDG and M-TACA are 6%, 18% and 24%, respectively. The difference in weight loss may be attributed to functional groups attached to the surface. When weight losses of M-NMDG and M-TACA were compared it was found that M-TACA lost 6% more weight than M-NMDG. The more weight loss of M-TACA indicates that it has more flammable organic species in its structure. When M-NMDG and M-TACA are compared, it is clear that more NMDG is attached to the surface of M-TACA. This is also consistent with experimental results in boron sorption studies.

The FT-IR spectra of M, M-NMDG and M-TACA nanoparticles are given in Fig. 1-D. The spectra strongly confirm the presence of severe peak Si-O-Si bonds at 1072 cm^{-1} characteristic for M-SiO_2 nanoparticles (Fig S4). In addition, the peak at 799 cm^{-1} corresponds to the asymmetric stretches of Si-O-Si bonds. The band at 567 cm^{-1} confirms the presence of the Si-O-Fe bond (Fig S4). The peak at 949 cm^{-1} is due to the tensile vibration of the Si-O bond. Peaks at 3263 cm^{-1} and at 1634 cm^{-1} show the tensile, bending and vibration peaks of O-H (Fig S4) (Ma et al., 2012). As seen from the FT-IR spectrum of M-NMDG (Fig. 1-D and Fig S5), the band at 1468 cm^{-1} confirms the presence of the C-N bond. The absence of this peak in the infrared spectrum of M-SiO_2 obviously indicates that NMDG successfully binds to the surface (Foschiera et al., 2001; Ma et al., 2012; Madrakian et al., 2012). As seen in the FT-IR spectrum of M-TACA (Fig. 1-D and Fig S6), the broad band at 1649 cm^{-1} is estimated to cover both the tertiary amide C=O peak and the aromatic C=C. The aromatic N = N band at 1471 cm^{-1} and the aromatic C-N band at 1349 cm^{-1} confirms the presence of a tertiary amide bearing the aromatic 1,2,3-triazole ring. Peak at 2101 cm^{-1} is characteristic peak for azide confirming the presence of N_3 in the structure (Ranjan and Brittain, 2007). Large band at 3346 cm^{-1} is stretching band of the O-H bond and peak at 1409 cm^{-1} is bending peak of the O-H bond, band at 2951 cm^{-1} is stretching band of the C-H bond. The measured peak values are consistent with the values given in the literature, indicating that NMDG is successfully functionalized via click chemistry (Ma et al., 2012; Ranjan and Brittain, 2007; Chen et al., 2010; Deng et al., 2011; Du et al., 2006; Joseph et al., 1987; Pretsch et al., 2000).

3.2. Sorption equilibrium

3.2.1. Effect of pH

The percent recovery (%) against the initial pH values of the M-NMDG and M-TACA sorbents is given in Fig. 1-E. As can easily be seen, the selectivity of the boron increased in the range of pH 8.5 and 9.0. The capacities of the sorbents increased up to an average pH of 9.2 and decreased after this value. The main reason for this observation is that the distribution of $B(OH)_3$ and $B(OH)_4^-$ in solution depends on the pH of the aqueous media. Boron can't ionize at pH 7 levels and at lower pH, it is found in neutral form ($B(OH)_3$). When pH increase to 9, the acceleration of ionization causes the borate anion to be dominated by $B(OH)_4^-$ (Nasef et al., 2014). For this reason, the pH value of the solution affects the boron sorption depending on the $B(OH)_3$ and $B(OH)_4^-$ distribution in solution (García-Soto and Muñoz Camacho, 2005) and at the pH range of 8.5–9, borate ion dominates.

3.2.2. Effect of dose

The dose studies for M-NMDG (Fig. 2-A) and M-TACA (Fig. 2-B) were carried out at the room temperature. 25 mL of boron solution was used in this study at pH 8.2.

From the curves in Fig. 2-A and Fig. 2-B, one can easily see that as the amount of sorbent increases, the sorption capacity (qe) decreases. This is because the active sites on the sorbent surface are not saturated by boron. As the amount of sorbent increases, (%) removal efficiency increases. The result is correlated with increased specific surface areas suitable for the sorption (Chen et al., 2010). As explained in many studies, this may be the case when a certain amount of sorbent is only able to quench a certain amount of boron (Bai et al., 2017). Boron concentration unchanged and increased amount of sorbent, so the boron concentration is reduced compared to the amount of sorbent in the aqueous medium. Therefore, sorbent is contacted with less boron ions, which means that it remains without saturating the active sites in the sorbent and mean that the active sites remain without being saturated in the sorbent. Therefore, there was a decrease in the value of the sorption (Bai et al., 2017), Furthermore, with increasing sorbent amount, stacking and clustering increases, thus, agglomeration is occurred so that the unit amount of sorbent total available surface overlap increases and the active specific surface areas are become narrow for the sorption. This situation is limiting the sorption capacity. It was found that active specific surface areas for the sorption are not saturated with the sorption (Bouguerra et al., 2008).

3.2.3. Effect of initial boron concentration

Influence of increasing initial boron concentrations on sorption capacities and (%) removal efficiencies of M-NMDG and M-TACA are given in Fig. 2-C. As the boron concentration increases, the sorption capacity increases and the (%) removal efficiencies decreases (Fig. 2-C). As can be seen in Fig. 2-C, the boron removal is highly rate dependent on the initial concentration. Increase of initial concentrations of boron and q_e values mainly affect the amount of borate ions that surround the active sites on the sorbent surface. As the initial boron concentrations increase, more borate ions are sprinkled into the sorbent surface (Chen et al., 2010) and for this reason borate ions are further sorptioned by sorbent. Despite the increase in initial concentration, the amount of sorbent remained constant, while the (%) removal efficiency reduced.

3.2.4. Effect of contact time

The effect of contact time on removal of boron from aqueous media was studied by using M-NMDG and M-TACA at different initial concentrations of sorbate, while the pH and the temperature and the amount of sorbent remained constant. The effect of contact time (5–180 min) on the boron sorption at different concentrations for M-NMDG and M-TACA are given in Fig. 2-D, respectively. As shown in Fig. 2-D, the sorption capacity of boron on M-NMDG and M-TACA reached to equilibrium at 30 min. This equilibrium is sufficient to remove boron from the aqueous solutions with M-NMDG and M-TACA and to reach equilibrium. The increase in q_t in the first 30 min is due to the excess of active specific surface area (Bouguerra et al., 2008; Kumar and Kumaran, 2005; Vadivelan and Kumar, 2005) in the sorbent. After 30 min, the sorption has reached equilibrium due to saturation of the active surface areas suitable to the sorption.

3.3. Reusability of sorbents

In order to investigate reusability of the sorbents, (%) removal efficiency of boron from aqueous solutions was studied successively (Fig. 3). As expected, (%) removal efficiency of sorbents is reduced by repeated use of sorbents. The basic reason for this is that the sorbents undergo deformation when they are reused.

3.4. Sorption isotherms

The Langmuir, Freundlich and Dubinin-Radushkevich isoterms constants were given in Table 1. The highest correlation values for sorbents were obtained in Langmuir isotherms (R^2 = 0.998 for M-NMDG, R^2 = 0.996 for M-TACA). Therefore, boron sorption isotherms of M-NMDG and M-TACA have been found to be compatible with Langmuir isotherm. Langmuir isotherm compatibility shows that the surface of the sorbent is homogeneous and the surface is covered by a monolayer (Langmuir, 1916).

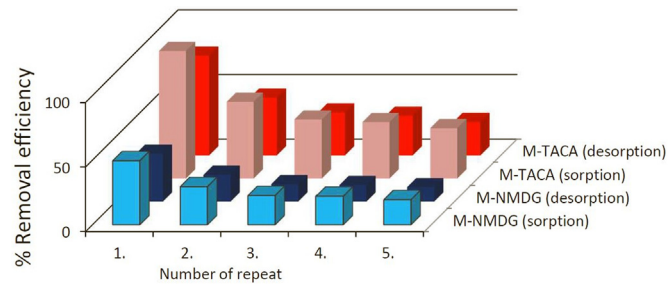

Fig. 3. Reusability of M-NMDG and M-TACA for boron sorption.

Table 1
Langmuir, Freundlich, Dubinin-Radushkevich isotherm constants of M-NMDG and M-TACA.

Modeller	İzoterm Sabitleri	M-SiO_2-NMDG	M-SiO_2-TACA
Langmuir İzotermi	Q_m (mg/g)	6688	13.44
	b (L/mg)	0.432	0.455
	R^2	0.998	0.996
Freundlich İzotermi	K_F [(mg/g)(mg/L)1/n]	2.99	2.21
	n	10.214	4.206
	R^2	0.702	0.974
Dubinin-Radushkevich İzotermi	q_{max} (mg/g)	1.413	1.177
	ε (Mol^2 KJ^{-2})	7.00E − 09	6.00E − 09
	E (KJ/mol)	8.451	9.128
	R^2	0.566	0.916

Dubinin–Radushkevich (D-R) isotherm was also applied to estimate the porosity apparent free energy and the characteristics of the sorption (Dubinin and Radushkevich, 1947). It can be used to describe sorption on both homogenous and heterogeneous surfaces. The extent of E is useful for guessing the type of sorption reaction. If E is in the range of 8–16 kJ/mol, sorption is ruled by chemical ion-exchange. In the case of E < 8 kJ/mol, physical forces may affect the sorption. The parameters obtained using above Eqs. (6)–(8) were evaluated in Table 1. The values calculated using Eq. (6) is 8.451 and 9.128 kJ/mol for the M-NMDG and M-TACA, respectively. This was indicating that chemical ion-exchange played a significant role in the sorption of the boron onto M-NMDG and M-TACA.

3.5. Sorption kinetics

Pseudo first-order and pseudo second-order kinetic modeling constants of the sorbents are given in Table 2. When the correlation coefficients of the kinetic modeling curves are considered, one can easily understand that the sorbents conform to the pseudo second order kinetic model for boron sorption. Table 2 also shows that $q_{e,\ exp}$ and $q_{e,\ cal}$ are compatible.

3.6. Comparison of sorption capacities of M-TACA with other sorbents

A comparison of boron sorption capacity of M-TACA with other designed NMDG sorbents reported in the literature (Ikeda et al., 2011; Inukai et al., 2004; Kaftan et al., 2005; Kamboh and Yilmaz, 2013; Li et al., 2011; Liu et al., 2009a; Qi et al., 2002; Wang et al., 2006) is given in Table 3. The data show that the sorption capacity of M-TACA is relatively high when compared with the common sorbents. It also has the advantage of magnetic separation.

Table 2
Pseudo-first order and pseudo-second order kinetic modeling constants of M-NMDG and M-TACA.

Sorbent	Concentration	Pseudo-first order				Pseudo-second order		
		$q_{e,,exp}$ (mg/g)	k_1 (min^{-1})	$q_{e,\ cal}$ (mg/g)	R^2	K_2 ($g\,mg^{-1}\,min^{-1}$)	$q_{e,,cal}$ (mg/g)	R^2
M-SiO_2-NMDG	8 ppm	3.302	0.0313	0.371	0.722	0.383	3.300	0.999
	16 ppm	4.653	0.0288	0.398	0.769	0.258	4.650	0.999
	32 ppm	6.453	0.183	0.632	0.917	0.198	6.459	0.999
M-SiO_2-TACA	8 ppm	6.585	0.0656	1.330	0.971	0.195	6.587	0.999
	16 ppm	9.367	0.0786	2.130	0.951	0.140	9.372	0.999
	32 ppm	10.127	0.0931	2.638	0.923	0.137	10.183	0.999

Table 3
Comparison of the boron sorption capacities of the various sorbents containing NMDG.

Polymer support (ab.)	Capacity (mg/g)	References
Glycidyl methacrylate-*co*-trimethylolpropane trimethacrylate (GMA-*co*-TRIM)	14.9	(Qi et al., 2002)
Cellulose	11.9	(Inukai et al., 2004)
Glucamine-modified MCM-41	8.65	(Kaftan et al., 2005)
Polyol-functionalized SBA-15	6.81	(Wang et al., 2006)
Tetraethoxysilane, (3-glycidoxypropyl) trimethoxysilane (TEOS-GPTMS)	12.4	(Liu et al., 2009b)
Silica-polyallylamine composites (SPC)	16.76	(Li et al., 2011)
6-Nylon fiber-GMA	12	(Ikeda et al., 2011)
Calyx 4 arene based magnetic sporopollenin	12.32	(Kamboh and Yilmaz, 2013)
M-TACA	13.44	In current study

4. Conclusion

In this work, NMDG-functionalized magnetic sorbents were synthesized using two different methods (direct coupling and click chemistry). The boron sorption capacities of the sorbents have been studied comparatively. Experimental parameters affecting sorption process such as boron concentration, contact time, sorbent amount and solution pH were investigated, and Langmuir and Freundlich and Dubinin-Radushkevich (D-R) adsorption isotherms models were applied. Percent removal efficiencies of M-NMDG and M-TACA are found to be 49.5% and 98.7%, respectively. The sorption capacities efficiencies of M-NMDG and M-TACA are found as 6.68 mg/g and 13.44 mg/g, respectively. Both M-NMDG and M-TACA have been found to be compatible with Langmuir isotherm, and the boron sorption kinetics conforms to the pseudo second order kinetics. The reusability study was carried out with five times boron sorption and desorption of M-NMDG and M-TACA sorbents. It is believed that the M-TACA sorbent is promising for efficient boron removal from aqueous media with high boron retention capacity and reusability properties. This study clearly demonstrates that functionalization with click chemistry is advantageous over the direct method of recycling by the boron magnetic separation method.

Acknowledgements

This project is funded by the financial support from Dicle University Research Fund (DUBAP, Project No. 13-ZEF-28, DUBAP, Project No. ZGEF.16.008).

Appendix A. Supporting information

Supplementary data associated with this article can be found in the online version at http://dx.doi.org/10.1016/j.ecoenv.2018.06.066.

References

Anastopoulos, I., et al., 2018. Use of nanoparticles for dye adsorption. J. Dispers. Sci. Technol. 39, 836–847.
Bai, C., et al., 2017. A novel method for removal of boron from aqueous solution using sodium dodecyl benzene sulfonate and D-mannitol as the collector. Desalination.
Benhammou, A., et al., 2005. Adsorption of metal ions onto Moroccan stevensite: kinetic and isotherm studies. J. Colloid Interface Sci. 282, 320–326.
Bhattacharya, A.K., Venkobachar, C., 1984. Removal of cadmium (II) by low cost adsorbents. J. Environ. Eng. 110, 110–122.
Bouguerra, W., et al., 2008. Boron removal by adsorption onto activated alumina and by reverse osmosis. Desalination 223, 31–37.
Cai, J., et al., 2007. Preparation and characterization of multiresponsive polymer composite microspheres with core–shell structure. Colloid Polym. Sci. 285, 1607–1615.
Chen, C.-Y., et al., 2011. Competitive biosorption of azo dyes from aqueous solution on the templated crosslinked-chitosan nanoparticles. J. Hazard. Mater. 185, 430–441.
Chen, J., et al., 2010. A versatile method for the preparation of end-functional polymers onto SiO 2 nanoparticles by a combination of surface-initiated ATRP and Huisgen [3+ 2] cycloaddition. Appl. Surf. Sci. 256, 2490–2495.
Deng, X., et al., 2011. Bio-orthogonal "Double-Click" chemistry based on multifunctional coatings. Angew. Chem. Int. Ed. 50, 6522–6526.
Devirian, T.A., Volpe, S.L., 2003. The Physiological Effects of Dietary Boron.
Du, G., et al., 2006. Characterization and application of Fe3O4/SiO2 nanocomposites. J. Sol-Gel Sci. Technol. 39, 285–291.
Dubinin, M., 1965. Modern state of the theory of volume filling of micropore adsorbents during adsorption of gases and steams on carbon adsorbents. Zh . Fiz. Khimii 39, 1305–1317.
Dubinin, M.M., Radushkevich, L., 1947. Equation of the characteristic curve of activated charcoal. Chem. Zentr. 1, 875.
Eggenhuisen, T., et al., 2013. Freeze-drying for controlled nanoparticle distribution in Co/SiO2 Fischer–Tropsch catalysts. J. Catal. 297, 306–313.
Foschiera, J.L., et al., 2001. FTIR thermal analysis on organofunctionalized silica gel. J. Braz. Chem. Soc. 12, 159–164.
Freundlich, H., 1906. Over the adsorption in solution. J. Phys. Chem. 57, 1100–1107.
Frey, N.A., et al., 2009. Magnetic nanoparticles: synthesis, functionalization, and applications in bioimaging and magnetic energy storage. Chem. Soc. Rev. 38, 2532–2542.
García-Soto, M. d.M. d.l.F., Muñoz Camacho, E.,, 2005. Boron removal by processes of chemosorption. Solvent Extr. Ion. Exch. 23, 741–757.
Gokce, Y., et al., 2014. Ultrasonication of chitosan nanoparticle suspension: influence on particle size. Colloids Surf. A: Physicochem. Eng. Asp. 462, 75–81.
Guan, Z., et al., 2016. Boron removal from aqueous solutions by adsorption—a review. Desalination 383, 29–37.
Ho, Y.-S., 2006. Review of second-order models for adsorption systems. J. Hazard. Mater. 136, 681–689.
Hong, R., et al., 2009. Double-miniemulsion preparation of Fe3O4/poly (methyl methacrylate) magnetic latex. J. Appl. Polym. Sci. 112, 89–98.
Hood, M.A., et al., 2014. Synthetic strategies in the preparation of polymer/inorganic hybrid nanoparticles. Materials 7, 4057–4087.
Ikeda, K., et al., 2011. Removal of boron using nylon-based chelating fibers. Ind. Eng. Chem. Res. 50, 5727–5732.
Inukai, Y., et al., 2004. Removal of boron (III) by N-methylglucamine-type cellulose derivatives with higher adsorption rate. Anal. Chim. Acta 511, 261–265.
Joseph, B.L., et al., 1987. Introduction to Organic Spectroscopy. Macmillan, New York.
Kaftan, Ö., et al., 2005. Synthesis, characterization and application of a novel sorbent, glucamine-modified MCM-41, for the removal/preconcentration of boron from waters. Anal. Chim. Acta 547, 31–41.
Kamboh, M.A., Yilmaz, M., 2013. Synthesis of N-methylglucamine functionalized calix [4] arene based magnetic sporopollenin for the removal of boron from aqueous environment. Desalination 310, 67–74.
Kantheti, S., et al., 2015. The impact of 1, 2, 3-triazoles in the design of functional

coatings. RSC Adv. 5, 3687–3708.
Kluczka, J., et al., 2015. Boron removal from water and wastewater using new polystyrene-based resin grafted with glycidol. Water Resour. Ind. 11, 46–57.
Kumar, K.V., Kumaran, A., 2005. Removal of methylene blue by mango seed kernel powder. Biochem. Eng. J. 27, 83–93.
Kyzas, G.Z., Matis, K.A., 2015. Nanoadsorbents for pollutants removal: a review. J. Mol. Liq. 203, 159–168.
Lan, F., et al., 2011. Facile synthesis of monodisperse superparamagnetic Fe3O4/PMMA composite nanospheres with high magnetization. Nanotechnology 22, 225604.
Langmuir, I., 1916. The constitution and fundamental properties of solids and liquids. Part I. Solids. J. Am. Chem. Soc. 38, 2221–2295.
Li, X., et al., 2011. Efficient removal of boron acid by N-methyl-D-glucamine functionalized silica–polyallylamine composites and its adsorption mechanism. J. Colloid Interface Sci. 361, 232–237.
Liebert, T., et al., 2006. Click chemistry with polysaccharides. Macromol. Rapid Commun. 27, 208–213.
Link, A.J., Tirrell, D.A., 2003. Cell surface labeling of escherichia c oli via copper (i)-catalyzed [3+ 2] cycloaddition. J. Am. Chem. Soc. 125, 11164–11165.
Liu, H., et al., 2009a. Boron adsorption by composite magnetic particles. Chem. Eng. J. 151, 235–240.
Liu, H., et al., 2009b. Boron adsorption by composite magnetic particles. Chem. Eng. J. 151, 235–240.
Liu, H., et al., 2009c. Boron adsorption using a new boron-selective hybrid gel and the commercial resin D564. Colloids Surf. A: Physicochem. Eng. Asp. 341, 118–126.
Ma, C., et al., 2012. Preparation and characterization of monodisperse core–shell Fe3O4@SiO2 microspheres and its application for magnetic separation of nucleic acids from E. coli BL21. J. Biomed. Nanotechnol. 8, 1000–1005.
Madrakian, T., et al., 2012. Application of modified silica coated magnetite nanoparticles for removal of iodine from water samples. Nano-Micro Lett. 4, 57–63.
Mandoli, A., 2016. Recent advances in recoverable systems for the Copper-Catalyzed Azide-Alkyne Cycloaddition Reaction (CuAAC). Molecules 21, 1174.
Nasef, M.M., et al., 2014. Polymer-based chelating adsorbents for the selective removal of boron from water and wastewater: a review. React. Funct. Polym. 85, 54–68.
Pretsch, E., et al., 2000. Structure Determination of Organic Compounds. Springer.
Qi, T., et al., 2002. Synthesis and borate uptake of two novel chelating resins. Ind. Eng. Chem. Res. 41, 133–138.
RĂILEANU, M., et al., 2007. The colloidal route of the sol-gel process-an alternative to produce Fe3O4-SiO2 nanocomposites. J. Optoelectron. Adv. Mater. 9, 1399–1402.
Ranjan, R., Brittain, W.J., 2007. Tandem RAFT polymerization and click chemistry: an efficient approach to surface modification. Macromol. Rapid Commun. 28, 2084–2089.
Sabarudin, A., et al., 2005. Synthesis of cross-linked chitosan possessing N-methyl-d-glucamine moiety (CCTS-NMDG) for adsorption/concentration of boron in water samples and its accurate measurement by ICP-MS and ICP-AES. Talanta 66, 136–144.
Samatya, S., et al., 2010. Comparative boron removal performance of monodisperse-porous particles with molecular brushes via “click chemistry” and direct coupling. Colloids Surf. A: Physicochem. Eng. Asp. 372, 102–106.
Samatya, S., et al., 2015. Boron removal from RO permeate of geothermal water by monodisperse poly (vinylbenzyl chloride-co-divinylbenzene) beads containing N-methyl-D-glucamine. Desalination 364, 75–81.
Seo, T.S., et al., 2003. Click chemistry to construct fluorescent oligonucleotides for DNA sequencing. J. Org. Chem. 68, 609–612.
Shah, A., et al., 2017. Deficiency and toxicity of boron: alterations in growth, oxidative damage and uptake by citrange orange plants. Ecotoxicol. Environ. Saf. 145, 575–582.
Sing, K., 1982. Adsorption, Surface Area and Porosity. Academic Press, London.
Singh, M.S., et al., 2016. Advances of azide-alkyne cycloaddition-click chemistry over the recent decade. Tetrahedron 72, 5257–5283.
Tural, B., 2010. Separation and preconcentration of boron with a glucamine modified novel magnetic sorbent. Clean–Soil Air Water 38, 321–327.
Tural, B., et al., 2013. Carboligation reactions mediated by benzoylformate decarboxylase immobilized on a magnetic solid support. Chirality 25, 415–421.
Tural, S., et al., 2016. Removal of hazardous azo dye Metanil Yellow from aqueous solution by cross-linked magnetic biosorbent; equilibrium and kinetic studies. Desalin. Water Treat. 57, 13347–13356.
Vadivelan, V., Kumar, K.V., 2005. Equilibrium, kinetics, mechanism, and process design for the sorption of methylene blue onto rice husk. J. Colloid Interface Sci. 286, 90–100.
Wang, B., et al., 2014. Removal technology of boron dissolved in aqueous solutions–a review. Colloids Surf. A: Physicochem. Eng. Asp. 444, 338–344.
Wang, L., et al., 2006. Novel organic–inorganic hybrid mesoporous materials for boron adsorption. Colloids Surf. A: Physicochem. Eng. Asp. 275, 73–78.
Wang, Q., et al., 2003. Bioconjugation by copper (I)-catalyzed azide-alkyne [3+ 2] cycloaddition. J. Am. Chem. Soc. 125, 3192–3193.
Wang, Y., et al., 2009. Synthesis and characterization of end-functional polymers on silica nanoparticles via a combination of atom transfer radical polymerization and click chemistry. React. Funct. Polym. 69, 393–399.
Werz, D.B., Seeberger, P.H., 2005. Carbohydrates as the next frontier in pharmaceutical research. Chem.-A Eur. J. 11, 3194–3206.
Xie, X., et al., 2015. Development and characterization of magnetic molecularly imprinted polymers for the selective enrichment of endocrine disrupting chemicals in water and milk samples. Anal. Bioanal. Chem. 407, 1735–1744.
Yang, T., et al., 2017. Superparamagnetic colloidal chains prepared via Michael-addition. Colloids Surf. A: Physicochem. Eng. Asp.